РОССИЙСКАЯ АКАДЕМИЯ НАУК

КОСМИЧЕСКИЕ ИССЛЕДОВАНИЯ

Главный редактор
Л.И. Седов

Dependence of Martian Magnetopause Shape and Its Dimensions on Solar Wind Dynamic Pressure according to *Phobos-2* Data

M. Verigin*, I. Apáthy**, G. Kotova*, J. Lemaire***, A. Remizov*, H. Rosenbauer****, K. Szegö**, J. Slavin*****, M. Tatrallyay**, K. Schwingenschuh******, and N. Shutte*

Space Research Institute, Russian Academy of Sciences, ul. Profsoyuznaya, 84/32 Moscow, 117810 Russia
**Central Research Institute for Physics, Budapest, Hungary*
***Institute of Aeronomie, Belgium*
****Max-Planck-Institut für Aeronomie, Katlenburg-Lindau, Germany*
*****NASA Goddard Space Flight Center, Greenbelt, Maryland, USA*
******Institut für Weltraumforschung, Graz, Austria*
Received December 5, 1995

Abstract—A semi-empirical model of the Martian magnetopause was developed according to data from the TAUS ion-spectrometer and the MAGMA magnetometer of the *Phobos-2* spacecraft for a period of solar activity maximum. The model describes a magnetopause position in the Martian magnetotail and a flaring angle depending on solar wind dynamic pressure ρV^2 as well as three points of magnetospheric boundary crossing on the dayside. The shape of the magnetopause is determined in the model from the pressure balance equation on this boundary. Both magnetic pressure and ionospheric plasma pressure are taken into account. A characteristic feature of the model is that the position of the magnetopause in the subsolar region is stable for rather large values of solar wind pressure ($\rho V^2 > 6 \times 10^{-9}$ dyn/cm^2).

INTRODUCTION

In spite of more than thirty years of Mars explorations (since *Mariner-4*, 1965) the intrinsic magnetic field of the planet is still not well, determined and the role of the ionosphere in interactions between the solar wind and the planet is not clear. Studies of variations of near planet plasma boundaries (the magnetopause and the bow shock) in response to solar wind dynamic pressure variations may bring us closer to a solution to these problems.

The authors of [1, 2] considered the position of the Martian bow shock in dependence on solar wind dynamic pressure near the terminator plane. However, it is impossible to make definite conclusions about the nature of flowed-around body, because the position of the bow shock depends on many other factors.

Gringauz *et al.* have qualitatively shown [3, 4] that the Martian magnetotail is compressed along with an increase in the solar dynamic pressure. Verigin *et al.* [5] performed a quantitative statistical analysis of this effect. A basic assumption of their analysis was a stable position of the magnetopause in the subsolar region. Later, Rosenbauer *et al.* [6] determined the average flaring angle for the magnetopause (the angle between the tangent to the magnetopause surface and incoming solar wind direction) in the region of its recording on circular orbits. Zhang *et al.* [7, 8] analyzed the dependence of this angle on solar wind dynamic pressure. These investigations provide some information on the shape of the planet's magnetopause.

A semiempirical model of the Martian magnetopause is presented in this work. This model agrees well with the magnetopause position in the magnetotail of Mars and an observed relationship between the flaring angle and solar wind dynamic pressure. It also well describes three available points of magnetopause measurement at the subsolar planet side.

INSTRUMENTATION AND EXPERIMENTAL DATA

The present model is based on solar wind proton measurements performed by the TAUS energy-spectrometer and magnetic field data measured by the MAGMA magnetometer on board *Phobos-2*. The TAUS spectrometer measured proton spectra within an energy range of 150 eV–6 keV every two minutes for a majority of Martian orbits in February–March 1989. The TAUS 'spectrometer had a field of view of ~40° × 40° centered on the aberration-corrected direction of the solar wind. The orbital motion of the planet causes this aberration. A more detailed description of the TAUS experiment is given in [9]. The MAGMA magnetometer had a range of ±100 nT, resolution
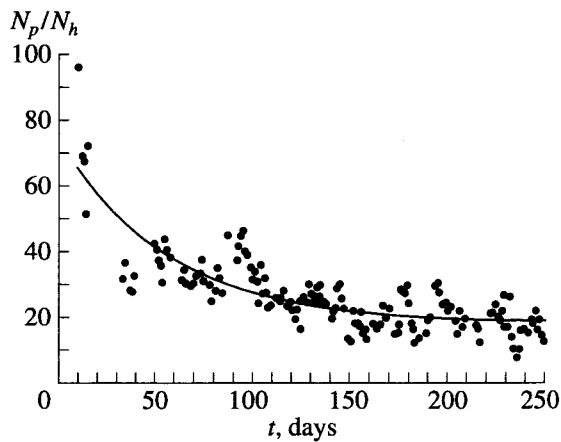
N_p/N_h

Fig. 1. The ratio of the proton channel daily average counts to the heavy ion channel daily average counts versus time starting from July 1, 1988.
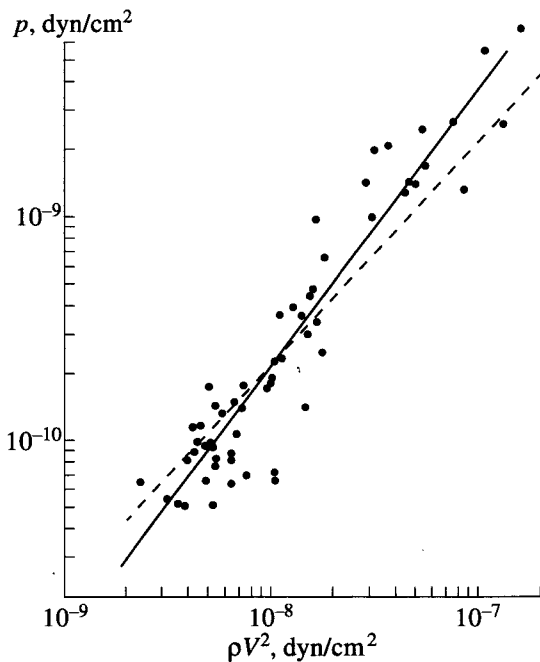
p, dyn/cm^2

Fig. 2. The sum of the thermal and magnetic pressures versus the solar wind dynamic pressure during the *Phobos-2* measurements.

surements were performed by both instruments in the undisturbed solar wind and in the Martian magnetotail. The crossings of the magnetopause near Mars were indicated by the disappearance of solar wind protons as measured by TAUS [11, 12] and by a simultaneous increase in the magnitude of the magnetic field (in the magnetotail region) or by a decrease of magnetic field turbulence (on the dayside) [13].

Measurements of absolute values of solar wind parameters and a knowledge of their experimental errors are very important to model the magnetopause shape. Unfortunately, the efficiency of proton detection by the TAUS instrument continuously decreased during the flight because an inlet aperture was not totally opened by the piezoelectric actuator [5]. To take this effect into account, the data were renormalized by a comparison of proton channel counts (N_p) with heavy ion channel counts (N_h) caused by penetration of some fraction of scattered protons to this channel (Fig. 1). An inlet aperture of the heavy ion channel was always open. A ratio of N_p/N_h has been fitted by the falling time exponent (solid line in Fig. 1); however, the dispersion of the experimental points is rather large and, so, there is still considerable ambiguity in the corrected data.

The TAUS experiment data should correlate with other satellite data published regularly in special catalogs. For this reason, we compared our data with data of the *IMP-8* satellite from the near Earth elliptical orbit. This comparison was done for a time interval when both spacecraft and the Sun were aligned. The TAUS data should be multiplied by a total correction factor of 2.2 at the end of active satellite life.

Values of the velocity V, the renormalized density n_p and the solar wind proton temperature T_p obtained from the TAUS experiment, and values of the magnetic field magnitude B from the MAGMA experiment were used to calculate the dynamic (ρV^2) and sum of the thermal and magnetic pressures of the solar wind (p):

$$\rho V^2 \approx n_p m_p V^2 (1 + n_\alpha m_\alpha/n_p m_p),$$

$$p = n_p k T_p (1 + n_\alpha T_\alpha/n_p T_p \qquad (1)$$

$$+ (1 + 2n_\alpha/n_p)T_e/T_p) + B^2/8\pi,$$

where the proton mass is n_p, the α subscript corresponds to alpha-particles, and the electron temperature is T_e. In our calculations we used solar wind parameters measured about 30 min before or after the spacecraft crossed the near-planet bow shock for entries to, or exits from, the Martian magnetosphere, respectively [5]. These values were averaged over 20–30 min. Average relations between different solar wind parameters were assumed to be $n_\alpha/n_p = 0.047$, $T_\alpha/T_p = 4.9$ and $T_e/T_p = 1.9$ [14].

0.05 nT, and returned data at a rate of one vector in every 45 s [10].

During the active life of the spacecraft, magnetopause crossings were recorded by the TAUS and MAGMA instruments on three elliptical orbits with low pericenters ($h \approx 850$ km above the planet's surface) and on a number of circular orbits, quasi-synchronous with the orbit of the moon Phobos. In total, sixty-four magnetopause crossings were registered on circular orbits (excluding multi-crossings) when mea-

Figure 2 presents the dependence of the p value on ρV^2. Points correspond to calculations according to (1), and the solid line shows an approximation of this dependence by a power law function:

$$p = 1.728(\rho V^2)^{1.232}. \qquad (2)$$

This function will be used to reduce a number of free parameters of the magnetopause model. The dashed line in Fig. 2 corresponds to the magnetosonic Mach number of ~4.6, which is typical for average solar wind conditions during measurements aboard *Phobos-2* [6].

MODEL OF THE MARTIAN MAGNETOPAUSE

An equation of pressure balance is commonly used for theoretical models of body shape flowed-around by the solar wind in the case of the induced as well as intrinsic magnetosphere [15, 16]. The left hand side of this equation always contains a dynamic solar wind pressure and in some cases its magnetic and thermal pressure. On the right hand side of the equation, there is a term describing the intrinsic planetary magnetic field pressure or the ionospheric plasma pressure. Because, for the Martian magnetosphere, both intrinsic magnetic field and ionospheric pressures may be important, there is a sum of these pressures on the right hand side of the equation used in our analysis:

$$k\rho V^2 \sin^2\alpha + p) = \begin{cases} \dfrac{4f^2M^2}{8\pi r^6} + p_0\exp(-(r-r_0)/H), \\ \qquad\qquad x > x^* \\ \dfrac{B^{*2}}{8\pi}\left(\dfrac{y^*}{y}\right)^4, \quad x < x^*, \end{cases} \qquad (3)$$

where $x = x_{\text{ase}}, y = \sqrt{y_{\text{ase}}^2 + z_{\text{ase}}^2}$ are the coordinates of a point on the magnetopause surface in the planetocentric aberrated solar-ecliptic coordinate system, the x_{ase} axis is assumed to be directed in the upstream solar wind direction; α is the magnetopause flaring angle, the angle between the x_{ase} axis and the magnetopause tangent in the plane containing x_{ase}; M is the planet's magnetic moment; p_0 is the pressure in the ionosphere at a distance r_0 from the planet center; H is the scale of ionospheric height; and $k \approx 0.88$ (for the adiabatic exponent $\gamma = 5/3$ and $f \approx 1.22$ ($f^2/k \approx 1.69$). The k coefficient describes a pressure transfer on the magnetopause near the subsolar point and the f coefficient reflects an increase in the magnetic field near the magnetopause caused by surface currents [15, 17].

Replacing $\sin^2(\alpha)$ by the derivative dy/dx, equation

(3) is transformed to

$$k\rho V^2 \frac{(dy/dx)^2}{1 + (dy/dx)^2} + p(\rho V^2)$$

$$= \begin{cases} \dfrac{4f^2M^2}{8\pi r^6} + p_0\exp(-(r-r_0)/H), \quad x > x^* \\ \dfrac{B^{*2}}{8\pi}\left(\dfrac{y^*}{y}\right)^4, \quad x < x^*, \end{cases} \qquad (4)$$

where $p(\rho V^2)$is used according to (2). A conservation of the magnetic flux in the magnetotail lobes ($x \le x^* \le 0$) is assumed in equations (3) and (4). The B^* and y^* parameters provide the continuity and smoothness of the magnetospheric surface at the point $x = x^*$. A value of $x^* = 0$ was used in our calculations. The magnetopause shape determined from equation (4) for a pure magnetic body coincides with a "realistic magnetopause" shape from the Tsyganenko model [18]. This model is based on statistically rich studies [19, 20]. The relation between the magnetotail width, distance to the magnetopause in the terminator plane and the distance to the subsolar point for the realistic magnetopause is 2.58 : 1.34 : 1, but for the magnetopause described by equation (4) it is 2.42 : 1.34 : 1.

If one assumes the magnetic moment of Mars M, the ionospheric pressure p_0 and the height scale H, then equation (4) allows one to obtain the magnetopause position, and therefore, the distance between the observed point of magnetopause crossing and the expected magnetopause position for any measured value of dynamic solar wind pressure ρV^2. There is an inverse problem, the determination of parameters M, p_0, and H, for which the discrepancy between observed points of the magnetopause crossing and the expected magnetopause position is smallest for observed values of ρV^2.

The available experimental data do not currently permit us to solve the three dimensional problem of optimization, because there is not enough data on magnetopause position on the planet dayside. Actually, only three points of magnetopause crossing on the dayside determine values of p_0 and H, so small changes of the positions of these points lead to considerable changes in the H value. Therefore, we have assumed $H = 110$ km, which corresponds to the double scale of thermal oxygen scale height in the Moroz *et al.* "extreme" model of the Martian atmosphere [21]. This model was chosen because the *Phobos-2* measurements were performed during a period close to the solar activity maximum. The influence of H changes on estimates of other parameters will be considered below.

If the standard procedure for optimization of observed magnetopause crossing point deviations from corresponding model surfaces is used, then the influence of 64 crossings of the magnetotail will
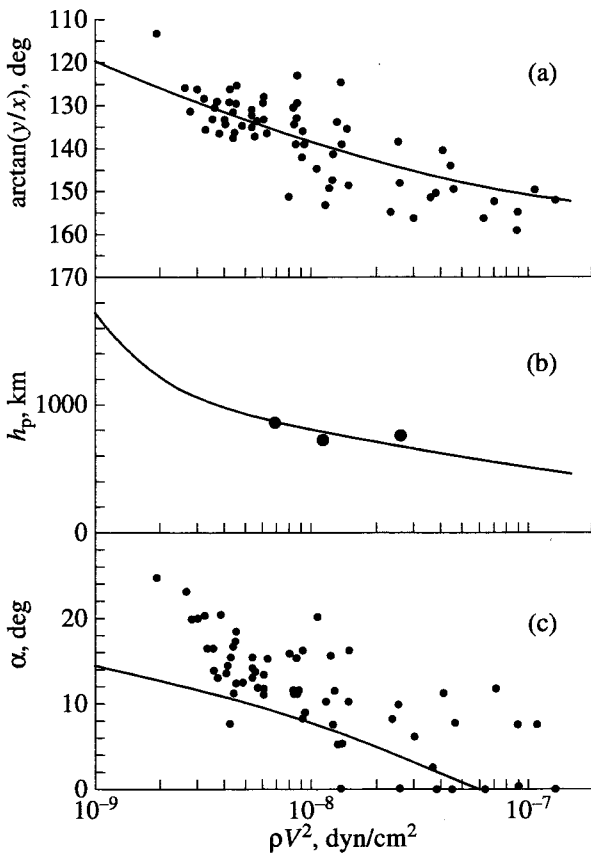
Fig. 3. A comparison of Mars magnetopause position obtained from model calculations ($M \sim 0.82 \times 10^{22}$ G cm³) with observed points of magnetopause crossing on (a) circular orbits and (b) elliptical orbits. A comparison of the theoretical magnetopause flaring angle with angles calculated using the *Phobos-2* measurements (c).

superpress the influence of three dayside crossings, which, however, are very important to model the subsolar magnetopause. To ensure an equal influence of the magnetopause observations on circular and elliptical orbits, values of M and p_0 were chosen that correspond to a minimum sum of mean-square deviations of the dayside magnetopause observations and mean-square deviations of the magnetotail boundary observations (normalized to the subsolar point).

Figure 3 presents results of the optimization of this model parameter ($M = 0.815 \times 10^{22}$ G cm³). Figure 3a shows the solar zenith angle [$\arctan(y/x)$] of magnetopause crossing points observed on circular orbits of *Phobos-2* versus the dynamic solar wind pressure. The solid line demonstrates the same dependence for the model magnetopause. Figure 3b shows a model dependence of magnetopause subsolar point height h_p on dynamic solar wind pressure by a solid line, and the points correspond to three day-time magnetopause crossings projected along model surfaces of magnetospheric boundary. It is clear from Figs. 3a and 3b that the model reasonably fits observed crossings of the Martian magnetopause and their dependence on ρV^2.

We performed calculations for different values of $H \neq 110$ km to clarify the influence of this parameter on M. Apparently, this influence can be disregarded because a change in scale height H from 50 to 200 km leads to insignificant changes in the magnetic moment M from 0.84×10^{22} to 0.79×10^{22} G cm³.

We have not considered the magnetopause angle. The magnetopause flaring angle α can be determined for any given magnetopause crossing and solar wind parameters ρV^2 and p by the formula [7, 22]

$$\sin^2\alpha = \frac{B_m^2/8\pi - p}{k\rho V^2}, \tag{5}$$

where the magnetic field magnitude in the Martian magnetotail B_m has been measured during time intervals when the magnetic field in the magnetotail lobes has become rather stable before or after magnetopause crossing. In the case of multiple magnetopause encounters, only the innermost crossings have been considered, so there are only innermost magnetopause crossings are presented in Fig. 3a (if it appeared that $B_m^2/8\pi < p$ then $\alpha = 0$ was plotted.)

Figure 3c presents the magnetopause flaring angle versus ρV^2. The observed angles (points) are above their model estimates by 5° on average. Changes in the model parameters M and p_0 do not lead to better agreement. Agreement may be achieved by changes of the model itself or by variations of measured plasma and/or magnetic field parameters, within possible experimental errors.

A change in the k value from $k \sim 0.66$ (the interplanetary magnetic field is antiparallel to the intrinsic magnetic field of the planet in the subsolar region, $\gamma = 2$) to $k = 2$ (a mirror reflection, $B = 0$, $T_p = 0$) in the equations (4) and (5) [23] corresponds to the first case. Three plots presented in Fig. 3 show reasonable agreement for $k = 1.5$ and $M = 0.98 \times 10^{22}$ G cm³. We will not discuss this opportunity in more detail here, because it contradicts the commonly accepted approach of magnetospheric boundary modeling.

A decrease in the magnetic field value by 10% would also lead to a reasonable fit of the observational data to the considered model for $M \sim 0.81 \times 10^{22}$ G cm³. In this case, the magnetopause flaring angles would come close to the practically unchanged model curve in Fig. 3c. However, in spite of some problems with a choice of zero level during the magnetic field measurements, the existence of such a systematic absolute experimental error is unlikely.

Total magnetic field of the magnetotail has been substituted in (5) to determine the flaring angle, but it seems reasonable that this equation should account only for the tangential component B_t to the magnetopause, but not the absolute value of the magnetic field. Zhang *et al.* [7, 8] showed a difference between the magnetopause flaring angle and the angle between the magnetic field direction in the magnetotail and the

sunward direction. However, it is necessary to replace B_m by $B_t \approx 0.85 \, B_m$ in (5) for reasonable model fitting of the dependence of magnetopause flaring angle on dynamic solar wind pressure that corresponds to the angle of ~30° between the magnetotail magnetic field direction and the tangent direction to the magnetopause. This value is considerably greater than ~14° (i.e. $B_t \sim 0.97 B_m$) estimated from the Phobos-2 data [7, 8].

One more reason for the discrepancy between flaring angles estimated from measurements and calculated according to the model is a possible error in the proton density measurements. As mentioned above, the scatter of points in Fig. 1 is rather large. Therefore, if we account for the time dependence of the N_p/N_h ratio by the approximation that goes 30% below the presented curve near its end, then the proton density determined with this new curve would be higher by about 40%.

An estimate of the proton density using the TAUS data may be reasonably enlarged by 20% if B_m in (5) would be simultaneously replaced by $B_t \sim 0.97 B_m$. After these changes, expression (2) becomes

$$p = 1.98(\rho V^2)^{1.246}. \qquad (6)$$

The optimization procedure of model parameters described above provides, in this case, an M value of 0.89×10^{22} G cm³. Figure 4 shows a comparison of this model with measurements applying the density correction by 20%. Now the constructed model fits the experimental data presented in all three figures reasonably well.

An asterisk in Fig. 4b marks the position of the magnetopause in the subsolar point calculated in [24] using plasma and magnetic field measurements on March 24, 1989. At that time, the Martian bow shock was observed aboard Phobos-2 in the subsolar region very far from the planet at a distance of ~2.8 Martian radii, which was connected with very low solar wind dynamic pressure $\rho V^2 \approx 10^{-9}$ dyn/cm² and the Alfvenic Mach number $M_A \approx 1.8$. The present model also describes this case well, so the pressure of the intrinsic planetary magnetic field is sufficient to decelerate the solar wind of very low dynamic pressure.

The shape of the model magnetopause similarly depends on ρV^2 in the cases presented in Figs. 3 and 4. Figure 5 presents boundaries of the Martian magnetosphere for different values of solar wind dynamic pressure calculated using (4) for the case of Fig. 4. The dashes in Fig. 5 were drawn through the points of spacecraft magnetopause crossing on different circular orbits. The angle of their inclination to the X axis is the magnetopause flaring angle α (5).

A characteristic feature of the model is that the position of the magnetopause in the subsolar region is practically invariable for $\rho V^2 \geq 6 \times 10^{-9}$ dyn/cm², while the magnetotail remains "compressible" up to very high pressures (Fig. 5). This feature of the model magnetopause justifies in a way an assumption of
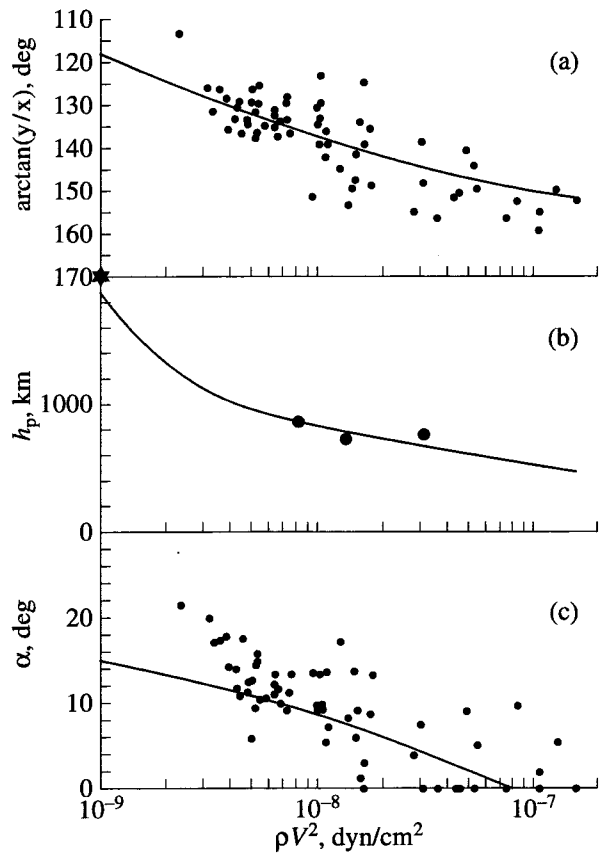

Fig. 4. A comparison of model results (M~0.82×10²² G cm³) with observed points of magnetopause crossing on (a) circular orbits and (b) elliptical orbits. A comparison of magnetopause flaring angles calculated using the equation (5), that contains the tangential magnetic field component $B_t \sim 0.97 B_m$ according to the Phobos-2 data, and accounting for density corrections of 20% (c).

Martian magnetopause stability in the subsolar region. The authors of [5] made this assumption considering the compressibility of the Martian magnetotail.

According to the model, the magnetic field pressure inside the magnetosphere $B^2/8\pi$ [the first term on the right hand side of (4)] is greater than the ionospheric pressure p_{ion} [the second term on the right hand side of (4)] over the entire magnetopause in the case of very low solar wind dynamic pressure. The ionospheric pressure becomes greater than the magnetic field pressure near the subsolar point if ρV^2 increases. However, the magnetic pressure is still greater for large zenith angles and far from the subsolar point, because it decreases rather slowly with distance from the planet as $\sim r^{-6}$ in comparison with ionospheric pressure decreasing $\sim \exp(-r/H)$. Figure 6 shows regions where the ionospheric pressure is greater or less than the magnetic pressure on the magnetopause. A dashed line corresponds to a case presented in Fig. 3, and a solid line, in Fig. 4. It can be
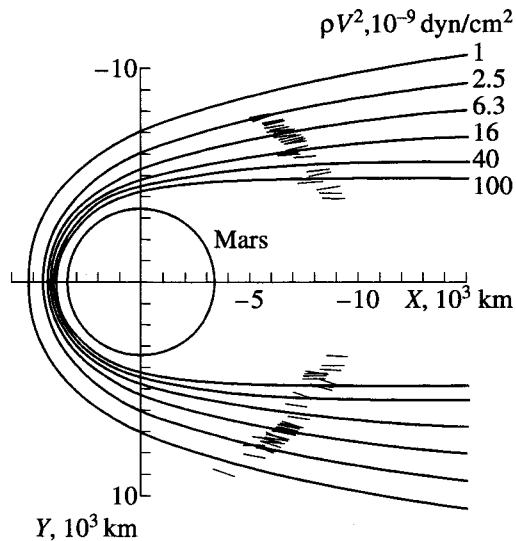
Fig. 5. Different shapes of the Martian magnetopause ($M \sim 0.89 \times 10^{22}$ G cm^3) corresponding to different values of solar wind dynamic pressure. The dashes are drawn through the points of spacecraft magnetopause crossing, the angle of their inclination to the X-axis is equal to a calculated value based on measurements of the magnetopause flaring angle.
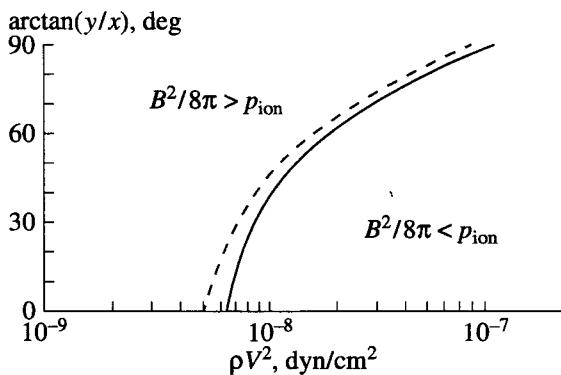

Fig. 6. Regions where either ionospheric pressure or magnetic pressure is dominant on the magnetopause for the models of Fig. 3 and Fig. 4.

seen from Fig. 6 that the magnetic pressure may be greater than the ionospheric pressure even for a very large solar wind dynamic pressure near the magnetopause for large zenith angles.

A dependence of subsolar point height on the solar wind dynamic pressure presented in Figs. 3b and 4b may be interpreted as the height profile of a sum of ionospheric and magnetic pressure in the subsolar magnetosphere multiplied by $1/k$. The exponential part of this curve at low heights describes the profile of ionospheric pressure. However, a question arises, whether electrons and ions in the Martian magnetosphere may produce the pressure more than $(1-3) \times 10^{-8}$ dyn/cm^2 at

700–800 km heights during the solar activity maximum.

There is no reliable information on the pressure distribution in the Martian ionosphere for the solar activity maximum. Because there are neither measurements of particle temperatures nor models of temperature distribution for this time period, Zhang and Luhmann [25] only estimated the lower limit of maximum ionospheric pressure of $(0.5-1.5) \times 10^{-8}$ dyn/cm^2 at the height of the maximum ionization and a zenith angle of $\sim75°$. According to the authors of [25], this estimate is the most unreliable result of their work. An extrapolation of this value to the subsolar region gives a pressure $\sim(1-3) \times 10^{-8}$ dyn/cm^2.

Even if the ionospheric pressure at a height of ~150 km was much higher than this lower limit during the *Phobos-2* observations, it is still unclear how such a high pressure can be kept near the magnetopause. This problem can be resolved if one assumes the existence of a plasma layer of temperature ≤10 eV and density ≤1000 cm^{-3}. The thickness of this layer should be about several hundred kilometers. The *Phobos-2* measurements provide some evidence of the existence of such a layer. Electric field measurements [26] show a decrease in electric field potential of the spacecraft to very low values after the dayside magnetopause crossing. This points to the existence of a dense plasma layer inside the magnetosphere. The plasma density ~700 cm^{-3} was measured by the Langmuir probe at heights of ~1000 km on February 8, 1989. However, data on plasma temperature are not available. The sensitivity of the radio occultation methods of electron density profile measurements (~1000 cm^{-3}) was not sufficient to discover such a plasma layer [28].

The present model of the Martian magnetopause is based on the pressure balance equation, which is chosen in such a way that the number of free parameters would be reduced to a minimum. Some a priori assumptions are a natural disadvantage of this approach. Unfortunately, it is impossible to propose a purely empirical model of the magnetopause for Mars, as has been done for the Earth [19, 20], because of a lack of observational data.

It should be pointed out that the magnetopause crossings, for which the model was created, were observed during the period close to the solar activity maximum and the corresponding height scale also was chosen. Therefore, this model should be modified for another period of the solar activity cycle.

The existence of the Martian intrinsic magnetic field can be justified only by direct measurements near the planet's surface. Our model only provides a new estimate of the planet's magnetic moment for the dipole field—$(0.8-1) \times 10^{22}$ G cm^3, which corresponds to the observed dependence of magnetopause position in the subsolar and tail regions on solar wind dynamic pressure and to a dependence of the magnetopause flaring angle on ρV^2.

Additionally, from a formal point of view, the curve shapes in Figs. 3b and 4b can be explained by the sum of two pressures, which vary according to the exponential law on the right hand sides of equations (3) and (4). However, this approach leads to unacceptably high pressures in the upper ionosphere.

The model of planet magnetopause shape can be applied, independent of the origin of the Martian magnetosphere, for studies of near planet bow shock variations and for further investigations of magnetic field distribution in the planet's magnetosphere.

CONCLUSION

The model of the Martian magnetopause was developed according to data of the TAUS ion-spectrometer and the MAGMA magnetometer of the *Phobos-2* spacecraft for a period of maximum solar activity.

The model simultaneously describes the magnetopause position observed in the Martian magnetotail and a flaring angle depending on solar wind dynamic pressure ρV^2 as well as three points of magnetospheric boundary crossing on the dayside.

The shape of the magnetopause is determined in the model according to the pressure balance equation on this boundary. Both magnetic pressure and ionospheric plasma pressure are taken into account. For a given solar wind dynamic pressure, the model gives a range of zenith angles for which the magnetic pressure near the magnetopause is higher than the ionospheric pressure.

The magnetic moment of Mars is one of free parameters of the model. It was determined by the least square method using the available points of magnetopause crossings and corresponding values of solar wind dynamic pressure. The obtained estimate $M = (0.8–1) \times 10^{22}$ G cm^3 practically does not depend on the choice of ionospheric height scale.

A characteristic feature of the model is that the position of the magnetopause in the subsolar region is nearly constant at $\rho V^2 > 6 \times 10^{-9}$ dyn/cm^2, while the magnetotail remains compressible up to extremely high values of solar wind pressure.

The model of planet magnetopause shape can be applied, independently of the origin of the Martian magnetosphere, as a basis for studies of near planet bow shock variations and for further investigations of the magnetic field distribution in the planet's magnetosphere.

ACKNOWLEDGMENTS

REFERENCES

1. Slavin, J.A., Holzer, R.E., Spreiter, J.R., *et al.*, Solar Wind Flow about the Terrestrial Planets. 2. Comparison with Gasdynamic Theory and Implications for Solar-Planetary Interactions, *J. Geophys. Res.*, 1983, vol. 88, no. A1, p. 19.

2. Schwingenschuh, K., Riedler, W., Zhang, T.L., *et al.*, The Martian Magnetic Field Environment: Induced or Dominated by an Intrinsic Magnetic Field?, *Adv. Space Res.*, 1992, vol. 12, no. 9, p. 213

3. Gringauz, K.I., Bezrukikh, V.V., Verigin, M.I., and Remizov, A.P., On Electron and Ion Component of Plasma in the Antisolar Part of Near-Martian Space, *J. Geophys. Res.*, 1976, vol. 81, no. 19, p. 3349.

4. Gringauz, K.I., Bezrukikh, V.V., Verigin, M.I., *et al.*, Measurements of Electron and Ion Plasma Components along the Mars-5 Satellite Orbit, *Space Research*, 1976, vol. 16, p. 1039.

5. Verigin, M.I., Gringauz, K.I., Kotova, G.A., *et al.*, The Dependence of the Martian Magnetopause and Bow Shock on Solar Wind Ram Pressure according to Phobos 2/TAUS Ion Spectrometer Measurements, *J. Geophys. Res.*, 1993, vol. 98, no. A2, p. 1303.

6. Rosenbauer, H., Verigin, M., Kotova, G., *et al.*, The Relationship between the Magnetic Field in the Martian Magnetotail and Upstream Solar Wind Parameters, *J. Geophys. Res.*, 1994, vol. 99, no. A9, p. 17199.

7. Zhang, T.L., Schwingenschuh, K., Russell, C.T., *et al.*, Martian Magnetotail Properties as Observed by the Phobos 2 Spacecraft, *Geophys. Res. Letters*, 1994, vol. 21, no. 12, p. 1121.

8. Zhang, T.L., Schwingenschuh, K., Petrinec, S.M., *et al.*, Studies of the Draping and Flaring Angles of the Mars and Earth Magnetotails, *Adv. Space Res.*, 1995, vol. 16, no. 4, p. (4)99.

9. Rosenbauer, H., Shutte, N., Apathy, I., *et al.*, Study of Three Dimensional Distribution Functions of Main Solar Wind Ions: Protons and Alpha-Particles in the Project "Phobos". The TAUS Experiment (Complex MPK), in *Apparatura i metody issledovaniya kosmicheskogo prostranstva* (Instruments and Methods for Space Research), Moscow: Nauka, 1989, p. 30.

10. Aydogar, U., Schwingenschuh, K., Schelch, G., *et al.*, The Phobos Fluxgate Magnetometer (MAGMA) Instrument Description, *Preprint IWF-8904, Austrian Acad. Sci.*, 1989.

11. Rosenbauer, H., Shutte, N., Apathy, I., *et al.*, First Results of Measurements of Martian Origin Ions and Discovery of Plasma Layer in the Martian Magnetosphere according to Data of the TAUS Experiment aboard the Phobos-2 Spacecraft, *Pis'ma Astron. Zh.*, 1990, vol. 16, no. 4, p. 368.

12. Rosenbauer, H., Shutte, N., Apathy, I., *et al.*, Ions of Martian Origin and Plasma Sheet in the Martian Magnetotail: Initial Results of TAUS Experiment, *Nature*, 1989, vol. 341, no. 6243, p. 612.

13. Riedler, W., Mohlman, D., Oraevsky, V.N., *et al.*, Magnetic Field near Mars: First Results, *Nature*, 1989, vol. 341, no. 6243, p. 604.

14. Feldman, W.C., Asbridge, J.R., Bame, S.J., and Gosling, J.T., Plasma and Magnetic Fields from the Sun, in

The Solar Wind Output and Its Variations, White O.R., Ed., Boulder: Colorado Associated Univ., 1977, p. 351.

15. Spreiter, J.R., Summers, A.L., and Alksne, A.Y., Hydromagnetic Flow around the Magnetosphere, *Planet. Space Sci.*, 1966, vol. 14, p. 223.

16. Spreiter, J.R., Summers, A.L., and Rizzi, A.W., Solar Wind Flow Past Nonmagnetic Planets—Venus and Mars, *Planet. Space Sci.*, 1970, vol. 18, p. 1281.

17. Slavin, J.A. and Holzer, R.E, The Solar Wind Interaction with Mars Revisited, *J. Geophys. Res.*, 1982, vol. 87, no. B12, p. 10285.

18. Tsyganenko, N.A., Modeling the Earth's Magnetospheric Magnetic Field Confined within a Realistic Magnetopause, *J. Geophys. Res.*, 1995, vol. 100, no. A4, p. 5599.

19. Sibeck, D.G., Lopez, R.E, and Roelof, E.C., Solar Wind Control of the Magnetopause Shape, Location and Motion, *J. Geophys. Res.*, 1991, vol. 96, p. 5489.

20. Roelof, E.C. and Sibeck, D.G., Magnetopause Shape as a Bivariate Function of the Interplanetary Magnetic Field B_z and Solar Dynamic Pressure, *J. Geophys. Res.*, 1993, vol. 98, p. 21421

21. Moroz, V.I., Kerzhanovich, V.V., and Krasnopol'skii, V.A., Work Model of the Mars Atmosphere for the Mars-94 (MA-90) Project, *Kosm. Issled.*, 1991, vol. 29, no. 1, p. 3.

22. Petrinec, S.M. and Russel, C.T., An Empirical Model of the Size and Shape of the Near-Earth Magnetotail, *Geophys. Res. Letters*, 1993, vol. 20, no. 23, p. 2695.

23. Schield, M.A., Pressure Balance between Solar Wind and Magnetosphere, *J. Geophys. Res.*, 1969, vol. 74, no. 5, p. 1275.

24. Slavin, J., Verigin, M., Gringauz, K., *et al.*, The Solar Wind Interaction with Mars: Phobos-2 Bow Shock Observations on 24 March 1989, in *Plasma Environments of Non-Magnetic Planets*, COSPAR Colloquia Series, vol. 4, T.I. Gombosi, Ed., Oxford: Pergamon, 1993, p. 279.

25. Zhang, M.S.G. and Luhmann, J.G., Comparison of the Peak Ionosphere Pressure at Mars and Venus with flaring Solar Wind Dynamic Pressure, *J. Geophys. Res.*, 1992, vol. 97, no. E1, p. 1017.

26. Pedersen, A., Nairn, C., Grard, R., and Schwingenschuh, K., Derivation of Electron Densities from Differential Potential Measurements Upstream and Downstream of the Bow Shock and in the Magnetosphere of Mars, *J. Geophys. Res.*, 1991, vol. 96, no. A7, p. 11243.

27. Grard, R., Pedersen, A., Klimov, S., *et al.*, First Measurements of Plasma Waves near Mars, *Nature*, 1989, vol. 341, no. 6243, p. 607.

28. Zhang, M.S.G., Luhmann, J.G., Kliore, A.J., and Kim, J., A Post Pioneer Venus Reassessment of the Martian Dayside Ionosphere as Observed by Radio Occultation Methods, *J. Geophys. Res.*, 1990, vol. 95, no. B9, p. 14829.